AGU PUBLICATIONS

Geophysical Research Letters

RESEARCH LETTER
10.1002/2015GL063036

Key Points:
- A new seismicity model is proposed to detect possible earthquake triggering
- The large intermediate earthquake occurred at tiny transient stress changes
- Cyclic fatigue due to passing surface waves may have triggered the earthquake

Supporting Information:
- Table S1 and Figure S1

Correspondence to:
M. Miyazawa,
miyazawa@rcep.dpri.kyoto-u.ac.jp

Citation:
Miyazawa, M. (2015), Seismic fatigue failure may have triggered the 2014 M_w7.9 Rat Islands earthquake, *Geophys. Res. Lett.*, *42*, 2196–2203, doi:10.1002/2015GL063036.

Received 15 JAN 2015
Accepted 28 FEB 2015
Accepted article online 4 MAR 2015
Published online 8 APR 2015
Corrected 29 June 2015

This article was corrected on 29 JUN 2015. See the end of the full text for details.

Seismic fatigue failure may have triggered the 2014 M_w7.9 Rat Islands earthquake

Masatoshi Miyazawa[1]

[1]Disaster Prevention Research Institute, Kyoto University, Uji, Kyoto, Japan

Abstract Seismic waves propagating from large earthquakes cause global transient stress changes capable of triggering other earthquakes at great distances. The study of such remote and dynamic triggering phenomena provides a better understanding of the mechanisms that generate earthquakes. I introduce an integrated seismicity model to stochastically evaluate the time intervals of consecutive earthquakes at global scales, making it possible to detect a pair of earthquakes possibly related to each other. I show a M_w7.9 intermediate-depth earthquake that occurred in the Rat Islands in 2014 is inferred to have been associated with a sequence of distant large ($M_w \geq 6.5$) earthquakes originating from the Kermadec Islands. The passage of seismic surface waves from the Kermadec events that produced small stress changes varying within at most 10 Pa at the hypocenter, probably caused a reduction in the fault's strength by cyclic fatigue and eventually triggered its failure during their passage.

1. Introduction

On 23 June 2014 (UTC), significant seismicity was recorded in the Kermadec and Rat Islands. A M_w6.9 earthquake (19:19 UTC) occurred in the Kermadec region, followed by moderate to large aftershocks, while a M_w7.9 intermediate-depth earthquake (20:53 UTC) occurred in the Rat Islands, the Aleutian Islands, about 9000 km due north of the Kermadecs, with a shallow dip angle at a depth of about 109 km within the subducting Pacific slab [e.g., *Ye et al.*, 2014] (Figure 1). The Kermadec earthquake sequence occurred before the Rat Islands event and included the M_w6.9 main shock, succeeded by M_w6.5 (19:22 UTC) and M_w6.7 (20:06 UTC) events. According to the Global centroid moment tensor (CMT) catalog, their focal mechanisms are consistent with the observed orientation of the fault plane, which is aligned parallel to the subducting Pacific Plate, along the Kermadec trench. The Rat Islands event occurred during the passage of seismic surface waves propagating from the M_w6.7 Kermadec aftershock and was delayed from the arrival of the peak wave amplitude (Figure 2a). The time interval between the origin times of these two events is less than 1 h, which appears anomalously short considering the global seismicity rate for large earthquakes, therefore, this raises the possibility of remote triggering. Previous examples of possible remote triggering include triggered seismicity concurrent with the passage of seismic waves [e.g., *West et al.*, 2005; *Miyazawa and Mori*, 2006] and evident increases in the seismicity rate following the passage of seismic waves [e.g., *Hill et al.*, 1993; *Velasco et al.*, 2008]. Despite the reporting of probable remote triggering subsequent to (i.e., delayed by minutes and hours to months) the passage of distant seismic waves with large amplitudes [e.g., *Gonzalez-Huizar et al.*, 2012; *Pollitz et al.*, 2012; *Gomberg*, 2013], there is no objective evidence to demonstrate such a correlation. In the present study I propose a new seismicity model to stochastically evaluate the time intervals between consecutive earthquakes at global scales when the seismicity rate varies with time. While previous studies have examined the global clustering of large earthquakes by statistical analyses [e.g., *Bufe and Perkins*, 2005; *Michael*, 2011; *Daub et al.*, 2012; *Parsons and Geist*, 2012; *Shearer and Stark*, 2012; *Ben-Naim et al.*, 2013], here the aims are to statistically detect pairs of earthquakes that are possibly related to each other and to discuss the physical remote-triggering process.

2. Integrated Seismicity Model

I introduce an integrated seismicity model that stochastically examines the possibility for a causal relationship between the Kermadec and Rat Islands earthquakes. The model includes seismicity in nonoverlapping areas and comprehensively explains the seismicity on the basis of point process models, which include the stationary Poisson model, the aftershock decay model following Omori-Utsu (OU) law, and/or the epidemic-type aftershock sequence (ETAS) model [*Ogata*, 1988]. The OU law is a nonstationary Poisson

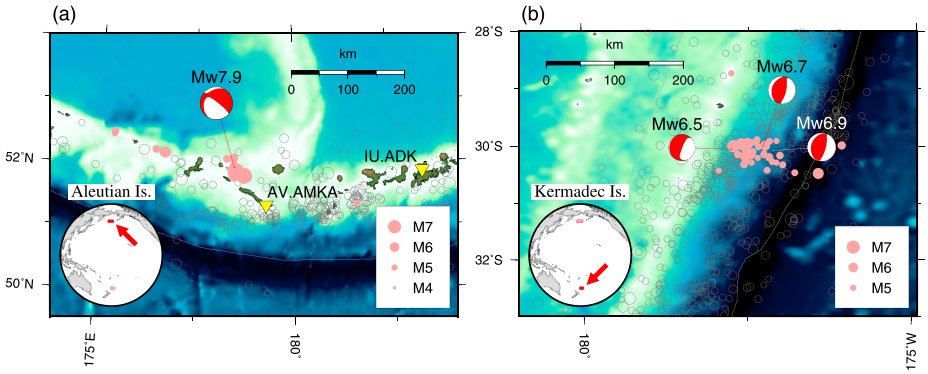

Figure 1. The study region and earthquake distributions. (a and b) Earthquake distributions in the Aleutian and Kermadec islands, from the IRIS catalog, and for the 100 day period after the M_w7.9 Rat Islands earthquake (23 June 2014 UTC). For the events referred to in the text, their focal mechanisms from the Global CMT catalog are also indicated. Earthquakes from 2000 to 23 June 2014 are indicated by gray circles. Inverted triangles show the positions of the seismic stations IU.ADK and AV.AMKA. Solid lines show plate boundaries [*Bird*, 2003].

process, in which all aftershocks are assumed to be affected by the main shock and the seismicity rate decays with time. The ETAS model is more versatile and includes the stationary Poisson process and the power law of the OU law. The seismicity rate, given by these models for a specific area A and earthquake magnitudes equal to or larger than M, which are usually larger than the completeness magnitude, as a function of time t, can be represented by

$$n(t|A,M) = \begin{cases} \mu \\ \dfrac{K}{(t+c)^p} \\ \mu + \displaystyle\sum_{l;t_l<t} \dfrac{K}{(t-t_l+c)^p} \exp\left(\alpha\left(M_l - M_0\right)\right) \end{cases}, \quad (1)$$

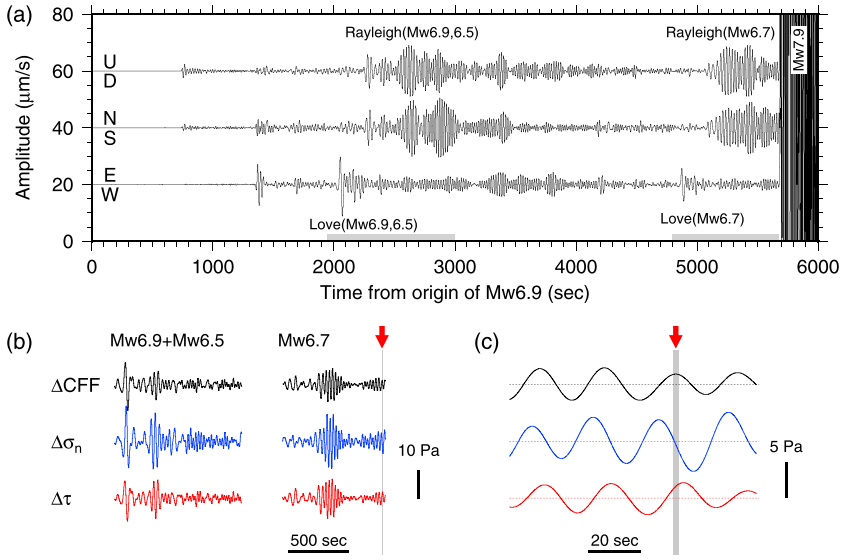

Figure 2. Observed seismic waveforms and stress changes. (a) Three seismic traces (0.005–0.05 Hz) representing the UD, NS, and EW components, recorded at the broadband station IU.ADK (see Figure 1). (b) Dynamic stress changes resolved for the M_w7.9 Rat Islands earthquake focal mechanism, at a depth of 109 km beneath stations IU.ADK and AV.AMKA. Station AV.AMKA was only used for analyses on the M_w6.7 Kermadec event, since some data were missing. The time windows used are shown in Figure 2a by gray bars. $\Delta\sigma_n$ represents the normal stress change (negative in compression), $\Delta\tau$ the shear stress change in the slip direction, and $\Delta\mathrm{CFF}(=\Delta\tau+\mu'\Delta\sigma_n)$ the Coulomb Failure Function change for a shear slip. The red arrows with gray bars indicate the origin time of the M_w7.9 event. (c) Stress changes magnified around the M_w7.9 event onset.

respectively, where μ, K, c, p, and α are parameters in each model, M_0 is the reference magnitude, and M_l is the earthquake magnitude at time t_l. The rate is zero when there are no data available. The cumulative number of earthquakes during a specific period T, from $t - T$ to t, is

$$N(t|A, M, T) = \int_T n(t|A, M)\, \mathrm{d}t. \tag{2}$$

If we assume that seismicities in areas modeled either by Poisson, OU, or ETAS are mutually independent, then the net seismicity in these areas can be represented as a function of time by a simple superposition of the models, appropriate to each area as follows:

$$N_{\mathrm{ism}}(t) = \sum_i N\left(t|A_i, M_i, T_i\right), \quad \text{where} \quad A_i \cap A_j = \emptyset \quad \text{for} \quad i \neq j. \tag{3}$$

This integrated seismicity model can represent the net seismicity at any scale. The model is applicable to any seismicity models with completeness magnitudes and periods of available data which vary in each area, regardless of the distances between them. Using this model, one can quantitatively evaluate time intervals between consecutive earthquakes, in terms of their corresponding probability.

The origin time of each earthquake that randomly follows the model shows a nonstationary Poisson distribution. This can be obtained by using equation (3), because the cumulative number corresponds to a time rescaling [e.g., *Brown et al.*, 2002] and is regarded as a stationary Poisson distribution for random data. Now consider the increase in the cumulative number ΔN during the time interval Δt from t, estimated from the model. An observation of m events during ΔN has a probability of

$$p(m, \Delta N) = \frac{1}{m!}(k\Delta N)^m \exp(-k\Delta N), \tag{4}$$

where k is the ratio of the total number of earthquakes to the model-predicted total number. Thus, the time interval Δt from a specific time t can be statistically quantified as a consequence of the time rescaling even though the seismicity rate varies with time. The probability that the interval of a single pair of consecutive earthquakes is within ΔN is

$$\begin{aligned} p(m \geq 1, \Delta N) &= 1 - p(0, \Delta N) \\ &= 1 - \exp(-k\Delta N). \end{aligned} \tag{5}$$

This also corresponds to the probability that, after an earthquake at time t, at least a single other earthquake occurs within Δt. Then the small probability means that the interval is stochastically short in terms of the integrated seismicity model.

To calculate the possibility of triggering an event in area A_0, due to events in areas A_i ($i = 1, 2, \ldots$), the magnitude of an earthquake modeled in A_i should be somewhat large, such that its seismic waves can trigger earthquakes in A_0. In the present case, $M \gtrsim 7$, which are presumably large enough to trigger other earthquakes around the world [*Velasco et al.*, 2008], is fixed in all areas, except the target area in the Aleutian Islands, where triggering is investigated. Also, a seismicity rate of zero can be assumed, by which the target earthquake in area A_0 occurs at time t_0, and the seismicity rate after the last earthquake in area A_i and before t_0 is zero, in order to only constrain the possibility of the triggered earthquake inside area A_0, following the triggering earthquake.

When the event in area A_0 is far from events in areas A_i, the traveltime of surface waves that contribute toward dynamic stress changes may be nonnegligible. The traveltime correction is possible simply due to equation (3)'s temporal increment for areas A_i. In the present study, a surface wave velocity of 4.5 km/s is used for the correction.

3. Results

3.1. Statistical Examinations

I first modeled global seismicity for $M \geq 6.7$ and $M \geq 6.9$ using the Incorporated Research Institutions for Seismology (IRIS) catalog for a 465 day time window, representing a year prior and 100 days posterior to the M_w7.9 Rat Islands earthquake, by adopting the ETAS model (Figure 3). The characteristic parameters for ETAS models are determined by the maximum likelihood method (Table S1 in the supporting information).

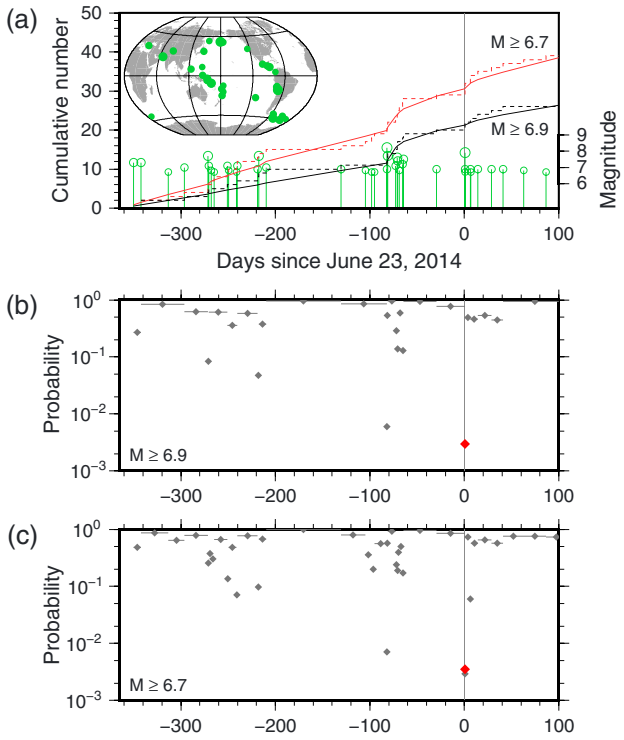

Figure 3. ETAS model and its estimated probabilities. (a) Global seismicity with $M \geq 6.7$ and for 465 days, including the 1 year and 100 day periods before and after the M_w7.9 Rat Islands earthquake. The cumulative earthquake number is shown by a broken line, and the model number predicted by the ETAS model is shown by a solid line. Black and red lines indicate the global seismicity for $M \geq 6.9$ and $M \geq 6.7$, respectively. (b and c) Probabilities estimated from the seismicity model in Figure 3a for pairs of consecutive earthquakes of $M \geq 6.9$ and $M \geq 6.7$, respectively. The values are shown by diamonds, with a line connecting the origin times of each pair of events. The probabilities for the paired Kermadec and M_w7.9 Rat Islands events are shown in red, and those of the other pairs are shown in gray.

The estimated probability that at least one earthquake of $M \geq 6.7$ occurs prior to the M_w7.9 event and following the M_w6.7 Kermadec event is 0.3799%, and the probability that at least one earthquake of $M \geq 6.9$ occurs prior to the M_w7.9 event and following the M_w6.9 Kermadec event is 0.2947%. These small values consequently indicates that there may exist a relationship between the consecutive events and the remote triggering due to $M \geq 6.7$ earthquake, whereas the estimation of these probabilities includes the possibility of aftershock in the Kermadec Islands.

Since this study focuses on the relationship between the earthquakes in the Kermadec and Aleutian islands, the global seismicity was also modeled for the Aleutian Islands and other global regions, using the integrated seismicity model under the null hypothesis of no relationship between seismicity in these areas (Figure 4). The submodel for the Aleutian Islands used $M \geq 5$, 6, and 7 events that locate between 47.90°N and 54.83°N latitude and 174.73°E and 165.54°W longitude and that for other global regions used $M \geq 6.7$ events, which may remotely trigger other events. For the submodel in the Aleutian Islands, ETAS models were adopted for $M \geq 5$ and 6 events and a Poisson model for $M \geq 7$ events, because only two $M \geq 7$ events were observed during this period (Table S1). When I assume there is no relationship between seismicity in the Aleutian Islands and other regions of the world, the probabilities obtained for the paired M_w6.7 Kermadec and M_w7.9 Rat Islands events, using models of $M \geq 5$, 6, and 7 in the Aleutian Islands and after travel time correction, are only 0.0444%, 0.0073%, and 0.0037%, respectively. Moreover, the probability is expected to become smaller for larger-magnitude earthquakes. Consequently, the occurrence of a M_w7.9 event in the Rat Islands, the Aleutian Islands at this specific timescale is stochastically very rare. The smallest value observed for the model using $M \geq 5$ events, in Figure 4b, is obtained for a sequence including a M6.1 deep (265 km depth) earthquake and a M5.7 shallow (37 km depth) event along the upper part of the subducting plate and for which their differences in epicentral distance and origin time are about 130 km and 1 s, respectively, thereby suggesting a pair of incidentally short interval.

In addition to the examination using the integrated seismicity model, a bootstrap analysis is performed to statistically assess this short time interval. I used 36 intervals between paired $M \geq 6.7$ events located outside the Aleutian Islands and $M \geq 6$ events located within the Aleutian Islands, as obtained from the IRIS catalog for a 5000 day time window that includes the 4900 day and 100 day periods before and after the M_w7.9 Rat Islands earthquake, respectively, and after correcting for surface wave travel times. These time intervals are shown to have an exponential distribution, as assessed using the Lilliefors test, where the probability of exceeding the maximum absolute difference between the empirical and theoretical distributions is ≥ 0.15.

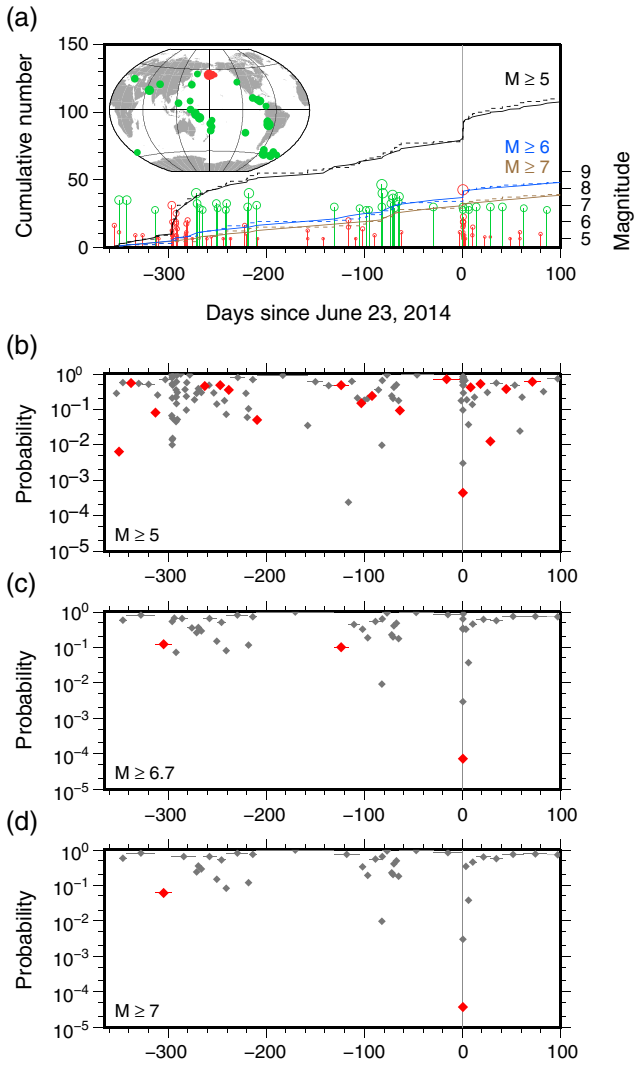

Figure 4. Integrated seismicity model and its estimated probabilities. (a) Integrated seismicity model for 465 days, including the 1 year and 100 day periods before and after the M_w7.9 Rat Islands earthquake. Earthquakes in the Aleutian Islands ($M \geq 5$) are in red, and those in the other regions of the world ($M \geq 6.7$) are green, both for the diagram and the inset map. The cumulative number is shown by a broken line and the model-predicted number by a solid line. The models used for the Aleutian Islands, when $M \geq 5$, 6, and 7, are in black, blue, and brown, respectively. (b–d) Probability of the occurrence of a pair of consecutive earthquakes, estimated from the integrated seismicity model with $M \geq 5$, 6, and 7 events, respectively. The values are shown by diamonds, with a line connecting the origin times of each pair of events, whereby those for the paired Kermadec and Aleutian events, after traveltime correction, are shown in red, and those for the other pairs, before correction, are in gray.

The estimated statistical population means after 1000 bootstrap replications range from 7.239 to 14.819 days (98% confidence level). Therefore, when the exponential distribution is assumed, i.e., there is no interaction between events located outside and inside the Aleutian Islands, the probability that the time interval is shorter than that between the paired M_w6.7 Kermadec and M_w7.9 Rat Islands events is from 0.0619% to 0.1267%.

These probability values are too small to claim that the observed short time interval between the Kermadec and the M_w7.9 Rat Islands events is incidental, thereby suggesting that the null hypothesis of no seismicity interaction between different areas is rejected; consequently, a causal relationship may exist between them. As previously reported for moderate-size earthquakes [*Velasco et al.*, 2008], surface waves from large ($M > 7$) earthquakes can potentially result in enhanced seismicity worldwide. Hence, while there has been no evidence that such large events dynamically triggered $M > 5$ events [*Parsons and Velasco*, 2011], it might be far more reasonable to interpret the M_w6.7 Kermadec event, and probably also previous M_w6.9 and M_w6.5 events in this region, as having remotely triggered the M_w7.9 Rat Islands main shock, since the surface wave arrivals were concomitant with the onset time of the M_w7.9 event (Figure 2a).

3.2. Triggering Stresses Due to the Seismic Waves

This work examines the initial physical rupture process of the M_w7.9 Rat Islands event using a linear kernel approach that computes continuous waveforms spanning the full spectrum at depth [*Miyazawa and Brodsky*, 2008], adapted for various phase velocities of surface waves. Figures 2b and 2c show temporal changes in the stress at the M_w7.9 Rat Islands hypocenter, associated with the passage of seismic surface waves originating from the three large distant Kermadec events. These changes can even be obtained for the simultaneous arrivals of the surface waves from the M_w6.9 and M_w6.5 Kermadec events, due to the linear relationship between the observed and the estimated data. The observed data used are from two seismic stations, IU.ADK and AV.AMKA. The time windows are chosen when the particle motion analyses show the direct arrivals of the Love and Rayleigh waves. The dynamic changes in the Coulomb Failure Function (ΔCFF) are resolved for the M_w7.9 Rat Islands earthquake fault mechanism from the Global CMT (strike = 207°,

dip = 26°, rake = −13°) at a depth of 109 km beneath stations IU.ADK and AV.AMKA, and the ΔCFF varies within roughly 10 Pa when the Lame's parameters, λ and μ, are 66 GPa and the effective friction coefficient μ' is assumed to be 0.4 at the depth. After correcting for the traveltimes to compare the M_w7.9 origin time with traces of stress changes, the triggering stress at the origin time is found to be only ∼1 Pa, accounting for several seconds of uncertainty in the traveltime corrections due to errors in the source location and origin time. The volumetric strain values corresponding the wave amplitude envelope vary from 10^{-12} to 10^{-11}. These stress and strain changes are about 5–6 orders of magnitude smaller than values that are reported necessary for dynamic triggering [*Gomberg and Johnson*, 2005; *Hill and Prejean*, 2007; *Miyazawa*, 2011].

4. Discussion

It seems physically unconvincing to infer that stress changes as little as ∼1 Pa can directly trigger the M_w7.9 Rat Islands earthquake, since such tiny stress changes could happen any time due to, for example, smaller nearby earthquakes, large teleseismic events, and/or earth tides. The 2014 M_w8.1 Iquique earthquake that occurred about 83 days before the Rat Islands earthquake caused transient stress changes at its hypocenter that were 1 order of magnitude larger than those associated with the Kermadec events; however, the Iquique earthquake did not trigger the Rat Islands event. This may indicate that the Rat Islands source fault was not close to failure at the time of the Iquique earthquake. Since earth tides have occasionally been linked to earthquakes [e.g., *Tanaka et al.*, 2002; *Cochran et al.*, 2004], I obtained the changes in vertical displacement at the epicenter due to earth tides [*Matsumoto et al.*, 2001] (Figure S1), yielding a strain change of 10^{-9}, which reduces normal loading stress on the fault, during the arrivals of the surface waves. This value is much larger than those obtained from the passage of the surface waves, however, it shows a monotonic increase and the corresponding stress is much smaller than the stress drop for tectonic earthquakes. Evidently, the M_w7.9 Rat Islands event was ready to occur, primed by the background stress loading prior to the Kermadec event sequence.

Given that the preexisting larger stress changes, prior to the M_w7.9 event onset, did not manage to trigger its rupture, but assuming that the passage of the surface waves from the Kermadec events did, then the long duration of cyclic stress changes (of about 10 Pa) due to the latter should have played an important role, even though their amplitudes were very small. In the case of an earthquake triggered by transient stress changes, the reduction in the fault's strength is a reasonable mechanism when the stress cannot build up due to the passage of seismic waves, in order to achieve the yielding stress. On the other hand, fatigue failure can generally occur at a loading stress level much smaller than the static yield strength.

Therefore, I propose that a cyclic fatigue took place to effectively reduce the fault's strength, together with the tidal changes and long-term background stress loading, and that failure eventually started at the CFF's positive change (Figure 2c), which apparently was smaller than the previous changes. Since earthquakes and tremors can be remotely triggered in phase with passing seismic waves [e.g., *West et al.*, 2005; *Miyazawa and Mori*, 2006; *Miyazawa and Brodsky*, 2008; *Yukutake et al.*, 2013], then every cycle with a small amplitude has the potential to weaken a fault to some extent, and repeated stress loading might eventually cause its rupture. A fault weakening mechanism, due to fluid migration induced by transient stress changes, has been reported by a different approach that uses longer-term data and repeating earthquakes [*Taira et al.*, 2009], whereas here I highlight the possible importance of cyclic fatigue using short-term data. This mechanism can contribute to solving long-standing questions regarding delayed triggering. An alternative mechanism, based on the rate-state friction law, involves slip acceleration on a fault plane, where transient stress changes accelerate the rate of slip on the fault close to failure, and hence, an earthquake can occur earlier than expected due solely to the background stress loading; this is the so-called clock advance model [*Gomberg et al.*, 1997].

Small cyclic stress changes due to the passage of seismic waves emanating from large earthquakes are frequently generated within the crust and upper mantle worldwide, resulting in a high chance of triggering following a large earthquake, although only when enough stress has built up on the expecting fault and when an eventual earthquake is ready to occur. The results of this study argue against the existence of a simple triggering threshold that is exceeded by a stress or strain change. In addition, the global seismicity rate increases following large earthquakes, as reported previously [*Velasco et al.*, 2008; *Parsons et al.*, 2014], for which cyclic fatigue due to long coda durations of surface waves might play a role. Given the ability of

this mechanism to remotely trigger earthquakes by inducing small stress changes, it is necessary that future estimates of seismic hazards consider the risk of remote triggering, not only for natural earthquakes and volcanic eruptions but also for induced seismicity in industrial production or injection, a matter of great concern in our society today [*Lupi et al.*, 2013; *Keranen et al.*, 2014].

5. Conclusions

I proposed a new universal model for seismicity to quantitatively and stochastically evaluate time intervals between consecutive earthquakes, where the net seismicity rate can be represented as the simple sum of submodels, preferably for each area unless one assumes a seismicity interaction between separate, individual areas. Using this model, I showed that the M_w7.9 Rat Islands earthquake of 23 June 2014 was probably remotely triggered by the M_w6.7 Kermadec earthquake, which occurred about 50 min earlier and at a site located about 9000 km away. The present results showed that the triggering stress change was as little as ~1 Pa, about 5–6 orders of magnitude smaller than the earthquake dynamic triggering threshold reported previously, and this may not have directly triggered the M_w7.9 Rat Islands earthquake. Then I proposed that cyclic fatigue due to surface waves from the M_w6.7 Kermadec event and probably also previous M_w6.9 and M_w6.5 events in this region, might play a role. Given this mechanism, one cannot rule out the possibility of worldwide remote triggering, not only for natural earthquakes and volcanic eruptions but also for induced seismicity.

Acknowledgments

This analysis used the seismicity data and seismic waveform data from the IRIS Data Management Center (http://www.iris.edu/hq/). Figures were drawn using the Generic Mapping Tools [*Wessel and Smith*, 1991] and ETOPO1 data from NOAA [*Amante and Eakins*, 2009]. Earth tides were calculated by GOTIC2 [*Matsumoto et al.*, 2001]. Discussion with Jim Mori helped develop this study. I thank two anonymous reviewers for the thoughtful and critical comments that helped to improve the manuscript. This work was supported by a MEXT Grant-in-Aid for Scientific Research (C) 25400450.

The Editor thanks two anonymous reviewers for their assistance in evaluating this paper.

References

Amante, C., and B. W. Eakins (2009), ETOPO1 1 arc-minute global relief model: Procedures, data sources and analysis, *NOAA Tech. Memorandum NESDIS NGDC-24,* Natl. Geophys. Data Cent., NOAA, doi:10.7289/V5C8276M.

Ben-Naim, E., E. G. Daub, and P. A Johnson (2013), Recurrence statistics of great earthquakes, *Geophys. Res. Lett.*, *40*, 3021–3025, doi:10.1002/grl.50605.

Bird, P. (2003), An updated digital model of plate boundaries, *Geochem. Geophys. Geosyst.*, *4*(3), 1027, doi:10.1029/2001GC000252.

Brown, E. N., R. Barbieri, V. Ventura, R. E. Kass, and L. M. Frank (2002), The time-rescaling theorem and its application to neural spike train data analysis, *Neural Comput.*, *14*, 325–346, doi:10.1162/08997660252741149.

Bufe, C. G., and D. M. Perkins (2005), Evidence for a global seismic-moment release sequence, *Bull. Seismol. Soc. Am.*, *95*, 833–843, doi:10.1785/0120040110.

Cochran, E. S., J. E. Vidale, and S. Tanaka (2004), Earth tides can trigger shallow thrust fault earthquakes, *Science*, *306*, 1164–1166, doi:10.1126/science.1103961.

Daub, E. G., E. Ben-Naim, R. A. Guyer, and P. A. Johnson (2012), Are megaquakes clustered?, *Geophys. Res. Lett.*, *39*, L06308, doi:10.1029/2012GL051465.

Gomberg, J. (2013), Permanently enhanced dynamic triggering probabilities as evidenced by two M ≥ 7.5 earthquakes, *Geophys. Res. Lett.*, *40*, 4828–4833, doi:10.1002/grl.50933.

Gomberg, J., and P. Johnson (2005), Dynamic triggering of earthquakes, *Nature*, *473*, 830, doi:10.1038/437830a.

Gomberg, J., M. L. Blanpied, and N. M. Beeler (1997), Transient triggering of near and distant earthquakes, *Bull. Seismol. Soc. Am.*, *87*, 294–309.

Gonzalez-Huizar, H., A. A. Velasco, Z. Peng, and R. R. Castro (2012), Remote triggered seismicity caused by the 2011, M9.0 Tohoku-Oki, Japan earthquake, *Geophys. Res. Lett.*, *39*, L10302, doi:10.1029/2012GL051015.

Hill, D. P., and S. G. Prejean (2007), Dynamic triggering, in *Treatise on Geophysics*, vol. 4, edited by G. Schubert, pp. 257–291, Elsevier, Amsterdam.

Hill, D. P., et al. (1993), Seismicity remotely triggered by the magnitude 7.3 Landers, California, earthquake, *Science*, *260*, 1617–1623, doi:10.1126/science.260.5114.1617.

Keranen, K. M., M. Weingarten, G. A. Abers, B. A. Bekins, and S. Ge (2014), Sharp increase in central Oklahoma seismicity since 2008 induced by massive wastewater injection, *Science*, *345*, 448–451, doi:10.1126/science.1255802.

Lupi, M., E. H. Saenger, F. Fuchs, and S. A. Miller (2013), Lusi mud eruption triggered by geometric focusing of seismic waves, *Nat. Geosci.*, *6*, 642–646, doi:10.1038/ngeo1884.

Matsumoto, K., T. Sato, T. Takanezawa, and M. Ooe (2001), GOTIC2: A program for computation of oceanic tidal loading effect, *J. Geod. Soc. Jpn.*, *47*, 243–248.

Michael, A. J. (2011), Random variability explains apparent global clustering of large earthquakes, *Geophys. Res. Lett.*, *38*, L21301, doi:10.1029/2011GL049443.

Miyazawa, M. (2011), Propagation of an earthquake triggering front from the 2011 Tohoku-Oki earthquake, *Geophys. Res. Lett.*, *38*, L23307, doi:10.1029/2011GL049795.

Miyazawa, M., and E. E. Brodsky (2008), Deep low-frequency tremor that correlates with passing surface waves, *J. Geophys. Res.*, *113*, B01307, doi:10.1029/2006JB004890.

Miyazawa, M., and J. Mori (2006), Evidence suggesting fluid flow beneath Japan due to periodic seismic triggering from the 2004 Sumatra-Andaman earthquake, *Geophys. Res. Lett.*, *33*, L05303, doi:10.1029/2005GL025087.

Ogata, Y. (1988), Statistical models for earthquake occurrences and residual analysis for point processes, *J. Am. Stat. Assoc.*, *83*, 9–27.

Parsons, T., and E. L. Geist (2012), Were global M ≥ 8.3 earthquake time intervals random between 1900 and 2011?, *Bull. Seismol. Soc. Am.*, *102*, 1583–1592, doi:10.1785/0120110282.

Parsons, T., and A. A. Velasco (2011), Absence of remotely triggered large earthquakes beyond the mainshock region, *Nat. Geosci.*, *4*, 312–316, doi:10.1038/ngeo1110.

Parsons, T., M. Segou, and W. Marzocchi (2014), The global aftershock zone, *Tectonophysics*, *618*, 1–34, doi:10.1016/j.tecto.2014.01.038.

Pollitz, F. F., R. S. Stein, V. Sevilgen, and R. Bürgmann (2012), The 11 April 2012 east Indian Ocean earthquake triggered large aftershocks worldwide, *Nature*, *490*, 250–253, doi:10.1038/nature11504.

Shearer, P. M., and P. B. Stark (2012), Global risk of big earthquakes has not recently increased, *Proc. Natl. Acad. Sci. U.S.A.*, *109*, 717–721, doi:10.1073/pnas.1118525109.

Taira, T., P. G. Silver, F. Niu, and R. M. Nadeau (2009), Remote triggering of fault-strength changes on the San Andreas Fault at Parkfield, *Nature*, *461*, 636–640, doi:10.1038/nature08395.

Tanaka, S., M. Ohtake, and H. Sato (2002), Evidence for tidal triggering of earthquakes as revealed from statistical analysis of global data, *J. Geophys. Res.*, *107*(B10), 2211, doi:10.1029/2001JB001577.

Velasco, A. A., S. Hernandez, T. Parsons, and K. Pankow (2008), Global ubiquity of dynamic earthquake triggering, *Nat. Geosci.*, *1*, 375–379, doi:10.1038/ngeo204.

Wessel, P., and W. H. F. Smith (1991), Free software helps map and display data, *Eos Trans. AGU*, *72*, 441–446.

West, M., J. J. Sánchez, and S. R. McNutt (2005), Periodically triggered seismicity at Mount Wrangell, Alaska, after the Sumatra earthquake, *Science*, *308*, 1144–1146, doi:10.1126/science.1112462.

Ye, L., T. Lay, and H. Kanamori (2014), The 23 June 2014 M_w 7.9 Rat Islands archipelago, Alaska, intermediate depth earthquake, *Geophys. Res. Lett.*, *41*, 6389–6395, doi:10.1002/2014GL061153.

Yukutake, Y., M. Miyazawa, R. Honda, M. Harada, H. Ito, M. Sakaue, K. Koketsu, and A. Yoshida (2013), Remotely triggered seismic activity in Hakone volcano during and after the passage of surface waves from the 2011 M9.0 Tohoku-Oki earthquake, *Earth Planet. Sci. Lett.*, *373*, 205–216, doi:10.1016/j.epsl.2013.05.004.

Erratum

In the originally published version of this article, Figure 3 was missing hypocenters in the inset map, the legend of Figure 4 contained the expression "($M \geq 6$)" in place of the correct reading of "($M \geq 6.7$)", and in the supporting information, Table S1 parameters were incorrect. These errors have since been corrected, and this version may be considered the authoritative version of record.